

Constraints on Long-Period Planets from an L' and M band Survey of Nearby Sun-Like Stars: Modeling Results

A. N. Heinze

Steward Observatory, University of Arizona, 933 N Cherry Avenue, Tucson, AZ 85721-0065

`ariheinze@hotmail.com`

Philip M. Hinz

Steward Observatory, University of Arizona, 933 N Cherry Avenue, Tucson, AZ 85721-0065

`phinz@as.arizona.edu`

Matthew Kenworthy

Steward Observatory, University of Arizona, 933 N Cherry Avenue, Tucson, AZ 85721-0065

`mkenworthy@as.arizona.edu`

Michael Meyer

Steward Observatory, University of Arizona, 933 N Cherry Avenue, Tucson, AZ 85721-0065

`mmeyer@as.arizona.edu`

Suresh Sivanandam

Steward Observatory, University of Arizona, 933 N Cherry Avenue, Tucson, AZ 85721-0065

`suresh@as.arizona.edu`

Douglas Miller

Steward Observatory, University of Arizona, 933 N Cherry Avenue, Tucson, AZ 85721-0065

`dmliller@as.arizona.edu`

ABSTRACT

¹Observations reported here were obtained at the MMT Observatory, a joint facility of the University of Arizona and the Smithsonian Institution.

We have carried out an L' and M band Adaptive Optics (AO) extrasolar planet imaging survey of 54 nearby, sunlike stars using the Clio camera at the MMT. Our survey concentrates more strongly than all others to date on very nearby F, G, and K stars, in that we have prioritized proximity higher than youth. Our survey is also the first to include extensive observations in the M band, which supplemented the primary L' observations. These longer wavelength bands are most useful for very nearby systems in which low temperature planets with red IR colors (i.e. $H - L'$, $H - M$) could be detected. The survey detected no planets, but set interesting limits on planets and brown dwarfs in the star systems we investigated. We have interpreted our null result by means of extensive Monte Carlo simulations, and constrained the distributions of extrasolar planets in mass M and semimajor axis a . If planets are distributed according to a power law with $dN \propto M^\alpha a^\beta dM da$, normalized to be consistent with radial velocity statistics, we find that $\alpha = -1.1$ and $\beta = -0.46$, truncated at 110 AU, is ruled out at the 90% confidence level. With 90% confidence no more than 8.1% of stars like those in our survey have systems with three widely spaced, massive planets like the A-star HR 8799. Our observations show that giant planets in long-period orbits around sun-like stars are rare, confirming the results of shorter-wavelength surveys, and increasing the robustness of the conclusion.

Subject headings: planetary systems, techniques: IR imaging, instrumentation: adaptive optics, astrometry, binary stars

1. Introduction

Well over 200 extrasolar planets have now been discovered using the radial velocity (RV) method. The limited temporal baseline of radial velocity observations, and the need to observe for a complete orbital period to confirm the properties of a planet with confidence, currently limit RV planets to periods of about 10 years or less (Cumming et al. 2008; Butler et al. 2006). The masses of discovered planets range from just a few Earth masses (Bouchy et al. 2009) up to around 20 Jupiter masses (M_{Jup}). We note that a 20 M_{Jup} object would be considered by many to be a brown dwarf rather than a planet, but that there is no broad consensus on how to define the upper mass limit for planets. For a good overview of RV planets to date, see Butler et al. (2006) or <http://exoplanet.eu/catalog-RV.php>.

The large number of RV planets makes it possible to examine the statistics of extrasolar planet populations. Several groups have fit approximate power law distributions in mass and semimajor axis to the set of known extrasolar planets. Necessarily, however, these power laws are not subject to observational constraints at orbital periods longer than 10 years – and it is at these orbital periods that we find giant planets in our own solar system. We cannot obtain a good understanding of planets in general without information on long period extrasolar planets. Nor can we see how our

own solar system fits into the big picture of planet formation in the galaxy without a good census of planets in Jupiter- and Saturn-like orbits around other stars.

Repeatable detections of extrasolar planets (as opposed to one-time microlensing detections) have so far been made by transit detection, by RV variations, by astrometric wobble, or by direct imaging. Of these methods, transits are efficient only for detecting close-in planets. The RV method is currently limited (by the amount of time high-precision spectrographs have been operating) to planets with periods of about 10 years or less, but even as temporal baselines increase, long period planets will remain harder to detect due to their slow orbital velocities. The amplitude of a star’s astrometric wobble increases with the radius of its planet’s orbit, but decades-long observing programs are still needed to find long-period planets. Direct imaging is the only method that allows us to characterize long-period extrasolar planets immediately.

Direct imaging of extrasolar planets is technologically possible at present only in the infrared, based on the planets’ own thermal luminosity, not on reflected starlight. The enabling technology is adaptive optics (AO), which allows 6-10m ground-based telescopes to obtain diffraction limited IR images several times sharper than those from HST, despite Earth’s turbulent atmosphere. Theoretical models of giant planets indicate that such telescopes should be capable of detecting self-luminous giant planets in large orbits around young, nearby stars. The stars should be young because the glow of giant planets comes from gravitational potential energy converted to heat in their formation and subsequent contraction: lacking any internal fusion, they cool and become fainter as they age.

Several groups have published the results of AO imaging surveys for extrasolar planets around F, G, K, or M stars in the last five years (see for example Masciadri et al. (2005); Kasper et al. (2007); Biller et al. (2007); Lafrenière et al. (2007). Of these, most have used wavelengths in the 1.5-2.2 μm range, corresponding to the astronomical H and K_S filters (Masciadri et al. 2005; Biller et al. 2007; Lafrenière et al. 2007). They have targeted mainly very young stars. Because young stars are rare, the median distance to stars in each of these surveys has been more than 20 pc.

In contrast to those above, our survey concentrates on very nearby F, G, and K stars, with proximity prioritized more than youth in the sample selection. The median distance to our survey targets is only 11.2 pc. Ours is also the first survey to include extensive observations in the M band, and only the second to search solar-type stars in the L' band (the first was Kasper et al. (2007)). The distinctive focus on older, very nearby stars for a survey using longer wavelengths is natural: longer wavelengths are optimal for lower temperature planets which are most likely to be found in older systems, but which would be undetectable around all but the nearest stars. More information on our sample selection, observations, and data analysis can be found in our concurrently published Observations paper. Our Observations paper also details our careful evaluation of our survey’s sensitivity, including extensive tests in which fake planets were randomly placed in the raw data and then recovered by an experimenter who knew neither their positions nor their number. Such tests are essential for establishing the true relationship between source significance (i.e. 5σ , 10σ ,

etc.) and survey completeness.

Our survey places constraints on a more mature population of planets than those that have focused on very young stars, and confirms that a paucity of giant planets at large separations from sun-like stars is robustly observed at a wide range of wavelengths.

In Section 2, we review power law fits to the distribution of known RV planets, including the normalization of the power laws. In Section 3, we present the constraints our survey places on the distribution of extrasolar giant planets, based on extensive Monte Carlo simulations. In Section 4 we discuss the promising future of planet-search observations in the L' and especially the M band, and in Section 5 we conclude.

2. Statistical Distributions from RV Planets

Nearly 300 RV planets are known. See Butler et al. (2006) for a useful, conservative listing of confirmed extrasolar planets as of 2006, or <http://exoplanet.eu/catalog-RV.php> for a frequently-updated catalog of all confirmed and many suspected extrasolar planet discoveries.

The number of RV planets is sufficient for meaningful statistical analysis of how extrasolar planets are distributed in terms of their masses and orbital semimajor axes. The lowest mass planets and those with the longest orbital periods are generally rejected from such analyses to reduce bias from completeness effects, but there remains a considerable range (2-2000 days in period, or roughly 0.03-3.1 AU in semimajor axis for solar-type stars; and 0.3-20 M_{Jup} in mass) where RV searches have good completeness Cumming et al. (2008). There is evidence that the shortest period planets, or ‘hot Jupiters,’ represent a separate population, a ‘pileup’ of planets in very close-in orbits that does not follow the same statistical distribution as planets in more distant orbits (Cumming et al. 2008). The hot Jupiters are therefore often excluded from statistical fits to the overall populations of extrasolar planets, or at least from the fits to the semimajor axis distribution.

Cumming et al. (2008) characterize the distribution of RV planets detected in the Keck Planet Search with an equation of the form

$$dN = C_0 M^{\alpha_L} P^{\beta_L} d \ln(M) d \ln(P). \quad (1)$$

where M is the mass of the planet, P is the orbital period, and C_0 is a normalization constant. They state that 10.5% of solar-type stars have a planet with mass between 0.3 and 10 M_{Jup} and period between 2 and 2000 days, which information can be used to derive a value for C_0 given values for the power law exponents α_L and β_L . They find that the best-fit values for these are $\alpha_L = -0.31 \pm 0.2$ and $\beta_L = 0.26 \pm 0.1$, where the L subscript is our notation to make clear that these are the exponents for the form using logarithmic differentials.

In common with a number of other groups, we choose to represent the power law with ordinary differentials, and to give it in terms of orbital semimajor axis a rather than orbital period P :

$$dN = C_0 M^\alpha a^\beta dM da. \quad (2)$$

Where C_0 , of course, will not generally have the same value for Equations 1 and 2. Manipulating the two equations and using Kepler's Third Law makes it clear that

$$\alpha = \alpha_L - 1. \quad (3)$$

and

$$\beta = \frac{3}{2}\beta_L - 1. \quad (4)$$

The Cumming et al. (2008) exponents produce $\alpha = -1.31 \pm 0.2$ and $\beta = -0.61 \pm 0.15$ when translated into our form. The mass power law is well behaved, but the integral of the semimajor axis power law does not converge as $a \rightarrow \infty$, so an outer truncation radius is an important parameter of the semimajor axis distribution.

The excellent paper presenting the 2006 Catalog of Nearby Exoplanets (Butler et al. 2006) carefully describes a heterogenous sample of extrasolar planets detected by several different RV search programs. With appropriate caution, Butler et al. (2006) refrain from quoting confident power law slopes based on the combined discoveries of many different surveys with different detection limits and completeness biases (in contrast, the Cumming et al. (2008) analysis was restricted to stars in the Keck Planet Search, which were uniformly observed up to a given minimum baseline and velocity precision). Butler et al. (2006) do tentatively adopt a power law with the form of Equation 2 for mass only, and state that α appears to be about -1.1 (or -1.16, to give the exact result of a formal fit to their list of exoplanets). However they caution that due to their heterogeneous list of planets discovered by different surveys, this power law should be taken more as a descriptor of the known planets than of the underlying distribution. They do not quote a value for the semimajor axis power law slope β .

Based mostly on Cumming et al. (2008), but considering Butler et al. (2006) as helpful additional input, we conclude that the true value of the mass power law slope α is probably between -1.1 and -1.51, with -1.31 as a good working model. The value of the semimajor axis power law slope β is probably between -0.46 and -0.76, with -0.61 as a current best guess. The outer truncation radius of the semimajor axis distribution cannot be constrained by the RV results: surveys like ours exist, in part, to constrain this interesting number.

The only other result we need from the RV searches is a normalization that will allow us to find C_0 . We elect not to use the Cumming et al. (2008) value (10.5% of stars having a planet with

mass between 0.3 and 10 M_{Jup} and period between 2 and 2000 days), because this range includes the hot Jupiters, a separate population.

We take our normalization instead from the Carnegie Planet Sample, as described in Fischer & Valenti (2005). Their Table 1 (online only) lists 850 stars that have been thoroughly investigated with RV. They state that all planets with mass at least 1 M_{Jup} and orbital period less than 4 years have been detected around these stars. Forty-seven of these stars are marked in Table 1 as having RV planets. Table 2 from Fischer & Valenti (2005) gives the measured properties of 124 RV planets, including those orbiting 45 of the 47 stars listed as planet-bearing in Table 1. The stars left out are HD 18445 and HD 225261. We cannot find any record of these stars having planets, and therefore as far as we can tell they are typos in Table 1.

Since all planets with mass above 1 M_{Jup} and period less than 4 years orbiting stars in the Fischer & Valenti (2005) list of 850 may be relied upon to have been discovered, we may pick any sub-intervals in this range of mass and period, and divide the number of planets falling into these intervals by 850 to obtain our normalization. We selected the range 1-13 M_{Jup} in mass, and 0.3-2.5 AU in semimajor axis. Twenty-eight stars, or 3.29% of the 850 in the Fischer & Valenti (2005) list, have one or more planets in this range. Our inner limit of 0.3 AU excludes the hot Jupiters, and thus the 3.29% value provides our final normalization. We note that if we adopt the Cumming et al. (2008) best-fit power laws, and use the 3.29% normalization to predict the percentage of stars having planets with masses between 0.3 and 10 M_{Jup} and orbital periods between 2 and 2000 days, we find a value of 9.3%, which is close to the Cumming et al. (2008) value of 10.5%. The slight difference is probably not significant, but might be viewed as upward bias in the Cumming et al. (2008) value due to including the hot Jupiters. In any case we would not have obtained very different constraints if we had used the Cumming et al. (2008) normalization in our Monte Carlo simulations.

For comparison, among the other papers reporting Monte Carlo simulations similar to ours, Kasper et al. (2007) used a normalization of 3% for planets with semimajor axes of 1-3 AU and masses greater than 1 M_{Jup} . This is close to our value of 3.29% for a similar range. Lafrenière et al. (2007) and Nielsen et al. (2008) fixed α and β in their simulations, and let the normalization be a free parameter.

Juric & Tremaine (2007) provide a helpful mathematical description of the eccentricity distribution of known RV planets:

$$P(\epsilon) = \epsilon e^{-\epsilon^2/(2\sigma^2)}. \quad (5)$$

where $P(\epsilon)$ is the probability of a given extrasolar planet's having orbital eccentricity ϵ , e is the root of the natural logarithm, and $\sigma = 0.3$. We find that this mathematical form provides an excellent fit to the distribution of real exoplanet eccentricities from Table 2 of Fischer & Valenti (2005), so we have used it as our probability distribution to generate random eccentricities for the

Monte Carlo simulations we describe in Section 3 below.

3. Constraints on the Distribution of Planets

3.1. Theoretical Spectra

Burrows et al. (2003) present high resolution, flux-calibrated theoretical spectra of giant planets or brown dwarfs for ages ranging from 0.1-5.0 Gyr and masses from 1 to 20 M_{Jup} (these are available for download from <http://zenith.as.arizona.edu/~burrows/>). We have integrated these spectra to give absolute magnitudes in the L' and M filters used in Clío, and have found that the results can be reasonably interpolated to give the L' or M band magnitudes for all planets of interest for our survey. Baraffe et al. (2003) also present models of giant planets and brown dwarfs, pre-integrated into magnitudes in the popular infrared bands. These models predict slightly better sensitivity to low mass planets in the L' band and slightly poorer sensitivity in the M band, relative to the Burrows et al. (2003) models. We cannot say if the difference is due to the slightly different filter sets used (MKO for Clío vs. Johnson-Glass and Johnson for Baraffe et al. (2003)), or if it is intrinsic to the different model spectra used in Burrows et al. (2003) and Baraffe et al. (2003). We have chosen to use the Burrows et al. (2003) models exclusively herein, to avoid any errors due to the slight filter differences. Since the Burrows et al. (2003) models predict poorer sensitivity in the L' band, in which the majority of our survey was conducted, our decision to use them is conservative.

3.2. Introducing the Monte Carlo Simulations

In common with several other surveys (Kasper et al. 2007; Biller et al. 2007; Lafrenière et al. 2007) we have used our survey null result to set upper limits on planet populations via Monte Carlo simulations. In these simulations, we input our sensitivity data in the form of tabular files giving the sensitivity in apparent magnitudes as a function of separation in arcseconds for each star. Various features of our images could cause the sensitivity at a given separation to vary somewhat with position angle: to quantify this, our tabular files give ten different values at each separation, corresponding to ten different percentiles ranging from the worst to the best sensitivity attained at that separation. These files are described in detail in our Observations paper, and are available for download from <http://www.hopewriter.com/Astronomyfiles/Data/SurveyPaper/>

Each Monte Carlo simulation runs with given planet distribution power law slopes α and β , and a given outer truncation value R_{trunc} for the semimajor axis distribution. Using the normalization described in Section 2, the probability P_{plan} of any given star having a planet between 1 and 20 M_{Jup} is then calculated from the input α , β , and R_{trunc} . In each realization of our survey, each star is randomly assigned a number of planets, based on Poisson statistics with mean P_{plan} . In most cases $P_{plan} \ll 1$, so the most likely number of planets is zero. If the star turns out to have

Table 1. L' Band Absolute Mags from Burrows et al. (2003)

Planet Mass in M_{Jup}	Mag at 0.10 Gyr	Mag at 0.32 Gyr	Mag at 1.0 Gyr	Mag at 3.2 Gyr	Mag at 5.0 Gyr
1.0	19.074	23.010	27.870	33.50 ^a	35.50 ^a
2.0	16.793	19.351	23.737	28.398	29.479
5.0	14.500	16.397	18.588	22.437	24.407
7.0	13.727	15.390	17.336	20.131	21.574
10.0	12.888	14.437	16.246	18.480	19.466
15.0	12.00 ^b	13.61 ^b	14.773	16.816	17.691
20.0	11.30 ^b	12.98 ^b	14.190	15.967	16.766

^aNo models for these very faint planets appear in Burrows et al. (2003). We have inserted ad hoc values to smooth the interpolations. Any effect of the interpolated magnitudes for planets we could actually detect is negligible.

^bNo models for these bright, hot planets appear in Burrows et al. (2003), which focuses on cooler objects. We have added values from Baraffe et al. (2003) and then adjusted them to slightly fainter values to insure smooth interpolations.

Table 2. M Band Absolute Mags from Burrows et al. (2003)

Planet Mass in M_{Jup}	Mag at 0.10 Gyr	Mag at 0.32 Gyr	Mag at 1.0 Gyr	Mag at 3.2 Gyr	Mag at 5.0 Gyr
1.0	14.974	16.995	19.987	25.0 ^a	26.0 ^a
2.0	14.023	15.313	17.807	21.295	22.163
5.0	13.014	14.017	15.153	17.167	18.537
7.0	12.618	13.561	14.558	16.126	16.909
10.0	12.189	13.096	14.093	15.315	15.951
15.0	11.55 ^b	12.60 ^b	13.370	14.512	14.990
20.0	11.29 ^b	12.21 ^b	13.069	14.122	14.580

^aNo models for these very faint planets appear in Burrows et al. (2003). We have inserted ad hoc values to smooth the interpolations. Any effect of the interpolated magnitudes for planets we could actually detect is negligible.

^bNo models for these bright, hot planets appear in Burrows et al. (2003), which focuses on cooler objects. We have added values from Baraffe et al. (2003) and then adjusted them to slightly fainter values to insure smooth interpolations.

one or more planets, the mass and semimajor axis of each are randomly selected from the input power law distributions. The eccentricity is randomly selected from the Juric & Tremaine (2007) distribution, and an inclination is randomly selected from the distribution $P(i) \propto \sin(i)$. If the star is a binary, the planet may be dropped from the simulation at this point if the orbit seems likely to be unstable. In general we consider circumstellar planets to be stable as long as their apastron distance is less than 1/3 the projected distance to the companion star, and circumbinary planets to be stable as long as their periastron distance is at least $3\times$ greater than the projected separation of the binary. For planets orbiting low-mass secondaries, a smaller limit on the apastron distance is sometimes imposed, while often circumbinary planets required such distant orbits that they were simply not considered; the details are given in Table 4. For each planet passing the orbital stability checkpoint, a full orbit is calculated using a binary star code written by one of us (M. K.). The projected separation in asec is found, and the magnitude of the planet is calculated from its mass, distance, and age using the Burrows et al. (2003) models.

Finally, two random choices decide to what sensitivity value the planet’s predicted magnitude will be compared. First, one of the ten percentiles given in the sensitivity files is randomly selected. Then, it is determined at what significance level the planet must appear to be detected: 5σ , 7σ , or 10σ , where σ is a measurement of the PSF-scale noise in a given region of the image; see our Observations paper for details. Our blind sensitivity tests using fake planets placed in our raw data (again, see the Observations paper for details) showed that we could detect 97% of 10σ sources, 46% of 7σ sources, and 16% of 5σ sources. Accordingly, in our Monte Carlo simulations, there was a 16% chance that a planet would be evaluated against our 5σ sensitivity; failing that, there was a 30% chance it would be evaluated against our 7σ sensitivity. Failing that, the simulated planet was evaluated against our 10σ sensitivity.

Note that although we had 97% completeness at 10σ , we have elected to let all simulated planets be evaluated at least compared to 10σ , because at only slightly above 10σ the true completeness certainly becomes 100% for all practical purposes. Note that the random step deciding at what significance level to evaluate the planet is independent of what the actual brightness of the planet might be. For example, the 10σ sensitivity at a planet’s location might be $L' = 15.3$, in which case the planet would have a 16% chance of being evaluated against a sensitivity of $L' = 16.05$ (5σ), a 30% chance of being evaluated against $L' = 15.69$ (7σ), and a 54% chance of being evaluated against $L' = 15.3$. However, the simulated planet’s brightness could be anything: for example, $L' = 14.2$ (sure to be detected), or $L' = 19.8$ (sure to be undetected).

The low completeness (16%) at 5σ , as determined from our blind sensitivity tests using fake planets, may seem surprising. In these tests we distinguished between planets that were suggested by a concentration of unusually bright pixels (‘Noticed’), or else confidently identified as real sources (‘Confirmed’). Many more planets were noticed than were confirmed: for noticed planets, the rates are 100% at 10σ , 86% at 7σ , and 56% at 5σ . However, very many false positives were also noticed, so sources that are merely noticed but not confirmed do not represent usable detections. The completeness levels we used in our Monte Carlo simulations (16% at 5σ and 46% at 7σ)

refer to confirmed sources. No false positives were confirmed in any of our blind tests. Followup observations of suspected sources are costly in terms of telescope time, so a detection strategy with a low false-positive rate is important.

Though sensitivity estimators (and therefore the exact meaning of 5σ) differ among planet imaging surveys, ours was quite conservative, as is explained in our Observations paper. The low completeness we find at 5σ , which has often been taken as a high-completeness sensitivity limit, should serve as a warning to future workers in this field, and an encouragement to establish a definitive significance-completeness relation through blind sensitivity tests as we have done.

Note that our blind sensitivity tests, covered in our Observations paper, are completely distinct from the Monte Carlo simulations covered herein. The blind tests involved inserting a little over a hundred fake planets into our raw image data to establish our point-source sensitivity. In our Monte Carlo work we simulated the orbits, masses, and brightnesses of millions of planets, and compared them to our previously-established sensitivity limits to see which planets our survey could have detected.

3.3. A Detailed Look at a Monte Carlo Simulation

To evaluate the significance of our survey and provide some guidance for future work, we have analyzed in detail a single Monte Carlo simulation. We chose the Cumming et al. (2008) best fit values of $\alpha = -1.31$ and $\beta = -0.61$, with the semimajor axis truncation radius set to 100 AU. Planets could range in mass from 1 to 20 M_{Jup} . As described in Section 2 above, we normalized the planet distributions so that each star had a 3.29% probability of having a planet with semimajor axis between 0.3 and 2.5 AU and mass between 1 and 13 M_{Jup} . The simulation consisted of 50,000 realizations of our survey with these parameters.

In 38% of these simulated cases, our survey found zero planets, while 37% of the time it found one, and 25% of the time it found two or more. The planet distribution we considered in this simulation cannot be ruled out by our survey, since a null result such as we actually obtained turns out not to be very improbable.

The median mass of planets detected was 11.36 M_{Jup} , the median semimajor axis was 43.5 AU, the median angular separation was 2.86 asec, and the median significance was 21.4σ . This last number is interesting because it suggests that, for our survey, any real planet detected was likely to appear at high significance, obvious even on a preliminary, ‘quick-look’ reduction of the data. Therefore, such reductions should always be performed at the telescope, to allow immediate followup if a candidate is seen.

We suspected that there would be a detection bias toward very eccentric planets, because these would spend most of their orbits near apastron, where they would be easier to detect. This bias did not appear at any measurable level in our simulation. However, there was a weak but clear

bias toward planets in low-inclination orbits, which, of course, spend more of their time at large separations from their stars than do planets with nearly edge-on orbits.

A concern with any planet imaging survey is how strongly the results hinge on the best few stars. A survey of 54 stars may have far less statistical power than the number would imply if the best two or three stars had most of the probability of hosting detectable planets. Table 3 gives the percentage of planets detected around each star in our sample based on our detailed Monte Carlo simulation. Due to poor data quality, binary orbit constraints, or other issues, a few stars had zero probability of detected planets given the distribution used here. In general, however, the likelihood of hosting detectable planets is fairly well distributed.

In Table 4, we give the details of planetary orbital constraints used in our Monte Carlo simulations for each binary star we observed, complete with the separations we measured for the binaries. Note that HD 96064 B is a close binary star in its own right, so planets orbiting it were limited in two ways: the apastron could not be too far out, or the orbit would be rendered unstable by proximity to HD 96064 A – but the periastron also could not be too far in, or the binary orbit of HD 96064 Ba and HD 96064 Bb would render it unstable. Planets individually orbiting HD 96064 Ba or HD 96064 Bb were not considered in our survey, since to be stable the planets would have to be far too close-in for us to detect them. The constraints described in Table 4 account for most of the stars in Table 3 with few or no detections reported.

A final question our detailed simulation can address is how important the M band observations were to the survey results. In Table 5, we show that when M band observations were made, they did substantially increase the number of simulated planets detected.

Table 3. Percentage of Detected Planets Found Around Each Star

Star Name	% of Total Detected Planets	Median Mass	Median Semimajor Axis	Median Separation
GJ 117	6.07	7.66 M_{Jup}	39.36 AU	3.64 asec
ϵ Eri	5.83	6.98 M_{Jup}	18.26 AU	4.35 asec
HD 29391	5.80	8.14 M_{Jup}	49.13 AU	2.71 asec
GJ 519	4.74	10.44 M_{Jup}	40.51 AU	3.28 asec
GJ 625	4.67	9.72 M_{Jup}	29.18 AU	3.48 asec
GJ 5	4.45	9.60 M_{Jup}	53.42 AU	3.08 asec
BD+60 1417	3.95	11.58 M_{Jup}	44.48 AU	2.05 asec
GJ 355	3.81	9.71 M_{Jup}	53.91 AU	2.34 asec
GJ 354.1 A	3.67	9.58 M_{Jup}	60.12 AU	2.64 asec
GJ 159	3.57	9.73 M_{Jup}	57.95 AU	2.71 asec
GJ 349	3.35	11.38 M_{Jup}	44.40 AU	3.17 asec
61 Cyg B	3.29	11.32 M_{Jup}	19.53 AU	4.08 asec
GJ 879	3.03	11.18 M_{Jup}	36.84 AU	3.69 asec
GJ 564	2.94	10.67 M_{Jup}	56.80 AU	2.70 asec
GJ 410	2.93	12.78 M_{Jup}	41.83 AU	3.03 asec
GJ 450	2.89	12.90 M_{Jup}	38.72 AU	3.66 asec
GJ 3860	2.68	12.70 M_{Jup}	49.72 AU	2.69 asec
HD 78141	2.58	12.47 M_{Jup}	57.00 AU	2.24 asec
BD+20 1790	2.51	12.14 M_{Jup}	58.33 AU	2.02 asec
GJ 278 C	2.20	12.68 M_{Jup}	54.56 AU	3.04 asec
GJ 311	2.19	12.55 M_{Jup}	52.07 AU	3.20 asec
HD 113449	2.17	12.52 M_{Jup}	59.31 AU	2.29 asec
GJ 211	2.10	13.59 M_{Jup}	50.51 AU	3.30 asec
BD+48 3686	2.08	12.56 M_{Jup}	55.05 AU	2.01 asec
GJ 282 A	2.05	13.39 M_{Jup}	49.85 AU	2.99 asec
GJ 216 A	2.03	12.71 M_{Jup}	42.98 AU	4.21 asec
61 Cyg A	1.97	13.70 M_{Jup}	20.94 AU	4.54 asec
HD 1405	1.54	13.13 M_{Jup}	66.34 AU	2.04 asec
HD 220140 A	1.54	11.73 M_{Jup}	36.85 AU	1.73 asec
HD 96064 A	1.49	12.63 M_{Jup}	46.64 AU	1.75 asec
HD 139813	1.43	14.33 M_{Jup}	59.71 AU	2.37 asec
GJ 380	0.92	15.76 M_{Jup}	25.31 AU	4.21 asec

3.4. Monte Carlo Simulations: Constraining the Power Laws

The planet distribution we used in the single Monte Carlo simulation described above could not be ruled out by our survey. To find out what distributions could be ruled out, we performed Monte Carlo simulations assuming a large number of different possible distributions, parametrized by the two power law slopes α and β , and by the outer semimajor axis truncation radius R_{trunc} . Regardless of the values of α and β , each simulation was normalized to match the RV statistics of Fischer & Valenti (2005): any given star had 3.29% probability of hosting a planet with mass between 1 and 13 M_{Jup} and semimajor axis between 0.3 and 2.5 AU. The mass range for simulated planets was 1-20 M_{Jup} .

We tested three different values of α : -1.1, -1.31, and -1.51, roughly corresponding to the most optimistic permitted, the best fit, and the most pessimistic permitted values from Cumming et al. (2008). For each value of α , we ran simulations spanning a wide grid in terms of β and R_{trunc} . In contrast to the extensive results described in Section 3.3, the only data saved for these simulations was the probability of finding zero planets. Since we did in fact obtain a null result, distributions for which the probability of this was sufficiently low can be ruled out.

Figures 1 and 2 show the probability of a null result as a function of β and R_{trunc} for our three different values of α . Figure 1 presents constraints based on $\alpha = -1.31$, the best-fit value from RV statistics, while Figure 2 compares the optimistic case $\alpha = -1.1$ and the pessimistic case $\alpha = -1.51$. Each pixel in these figures represents a Monte Carlo simulation involving 15,000 realizations of our survey; generating the figures took several tens of hours on a fast PC. Contours are overlaid at selected probability levels. Regions within the 1%, 5%, and 10% contours can, of course, be ruled out at the 99%, 95%, and 90% confidence levels respectively. For example, we find that the most optimistic power laws allowed by the Cumming et al. (2008) RV statistics, $\alpha = -1.1$ and $\beta = -0.46$, are ruled out with 90% confidence if R_{trunc} is 110 AU or greater. Similarly, $\alpha = -1.51$ and $\beta = -0.3$, truncated at 100 AU, is ruled out. Though $\beta = 0.0$ is not physically plausible, previous work has sometimes used it as an example: for $\alpha = -1.31$, we rule out $\beta = 0.0$ unless R_{trunc} is less than 38 AU.

3.5. Model-Independent Constraints

It is also possible to place constraints on the distribution of planets without assuming a power law or any other particular model. To place such constraints, we performed an additional series of Monte Carlo simulations on a grid of planet mass and orbital semimajor axis. For each grid point we seek to determine a number $P(M, a)$ such that, with some specified level of confidence (e.g., 90%), the probability of a star like those in our sample having a planet with the specified mass M and semimajor axis a is no more than $P(M, a)$. We determine $P(M, a)$ by a search: first a guess is made, and a Monte Carlo simulation assuming this probability is performed. If more than 10% of the realizations of our survey turn up a null result, the guessed probability is too low; if less than

Table 3—Continued

Star Name	% of Total Detected Planets	Median Mass	Median Semimajor Axis	Median Separation
GJ 896 A	0.61	12.43 M_{Jup}	6.47 AU	0.98 asec
GJ 860 A	0.38	11.58 M_{Jup}	53.26 AU	6.62 asec
τ Ceti	0.38	17.19 M_{Jup}	25.49 AU	5.52 asec
GJ 896 B	0.34	11.40 M_{Jup}	6.78 AU	1.14 asec
ξ Boo B	0.32	12.07 M_{Jup}	8.25 AU	1.36 asec
HD 220140 B	0.28	12.04 M_{Jup}	25.92 AU	1.37 asec
ξ Boo A	0.24	12.89 M_{Jup}	8.72 AU	1.50 asec
GJ 659 B	0.21	17.71 M_{Jup}	62.54 AU	2.81 asec
GJ 166 B	0.17	16.12 M_{Jup}	6.19 AU	1.34 asec
GJ 684 A	0.17	14.93 M_{Jup}	85.98 AU	4.87 asec
HD 96064 B	0.13	14.43 M_{Jup}	38.55 AU	1.60 asec
GJ 505 B	0.12	15.94 M_{Jup}	17.11 AU	1.61 asec
GJ 166 C	0.10	15.56 M_{Jup}	6.43 AU	1.52 asec
GJ 505 A	0.07	16.32 M_{Jup}	18.08 AU	1.75 asec
GJ 702 A	0.02	15.90 M_{Jup}	6.21 AU	1.50 asec
GJ 684 B	None	NA	NA	NA
GJ 860 B	None	NA	NA	NA
GJ 702 B	None	NA	NA	NA
HD 77407 A	None	NA	NA	NA
GJ 659 A	None	NA	NA	NA
GJ 3876	None	NA	NA	NA
HD 77407 B	None	NA	NA	NA

Note. — This table applies to our detailed Monte Carlo simulation with 50,000 survey realizations run using $\alpha = -1.31$, $\beta = -0.61$, and semimajor axis truncation radius 100 AU. Of all the simulated planets that were detected, we present here the percentage that were found around each given star, and the median mass, semimajor axis, and projected separation for simulated planets found around each star. The table thus indicates around which stars our survey had the highest likelihood of detecting a planet. Many stars with poor likelihood are binaries, with few stable planetary orbits possible.

Table 4. Constraints on Simulated Planet Orbits Around Binary Stars

Star Name	separation (arcsec)	constraints on circumprimary apastron (arcsec/AU)	constraints on circumsecondary apastron (arcsec/AU)	constraints on circumbinary periastron (arcsec/AU)
HD 220140 AB	10.828	<3.61/71.3	<2.17/42.8	No Stable Orbits
HD 96064 AB	11.628	<3.88/95.6	<2.33/57.3	No Stable Orbits
HD 96064 Bab	0.217	No Stable Orbits	No Stable Orbits	>0.65/16.1
GJ 896 AB	5.366	<1.79/11.8	<1.79/11.8	No Stable Orbits
GJ 860 AB	2.386	<0.79/3.17	<0.60/2.41	>7.15/28.7
ξ Boo AB	6.345	<2.12/14.2	<2.12/14.2	No Stable Orbits
GJ 166 BC	8.781	<2.20/10.6	<2.20/10.6	No Stable Orbits
GJ 684 AB	1.344	<0.45/6.34	<0.27/3.80	>4.03/56.8
GJ 505 AB	7.512	<2.50/29.8	<2.50/29.8	No Stable Orbits
GJ 702 A	5.160	<1.76/8.85	<1.32/6.64	>15.9/79.7
HD 77407 AB	1.698	<0.57/17.2	<0.34/10.23	>5.11/153.7

Note. — Planets orbiting the primary in a binary star were considered to be de-stabilized by the gravity of the secondary if their apastron distance from the primary was too large. Similarly, planets orbiting the secondary had to have small enough apastron distances to avoid being de-stabilized by the primary. Circumbinary planets had to have a large enough periastron distance to avoid being de-stabilized by the differing gravitation of the two components of the binary. Note that HD 96064B is itself a tight binary star, so planets orbiting it had both a minimum periastron and a maximum apastron.

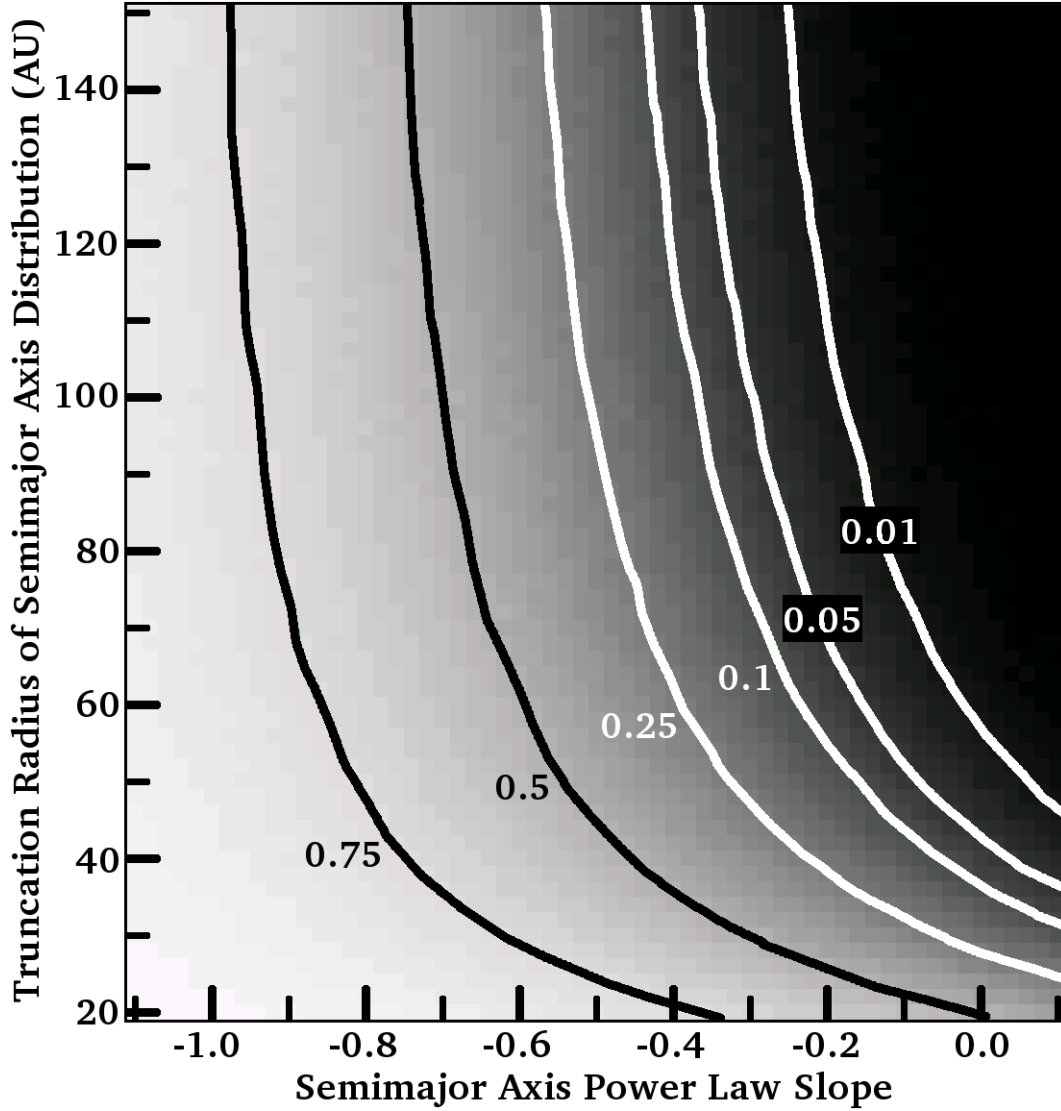


Fig. 1.— Probability of our survey detecting zero planets, as a function of the power law slope of the semimajor axis distribution β , where $\frac{dn}{da} \propto a^\beta$, and the outer truncation radius of the semimajor axis distribution. Here, the slope of the mass distribution α has been taken as -1.31, where $\frac{dn}{dM} \propto M^\alpha$. Since we found no planets, distributions that lead to a probability P of finding no planets are ruled out at the $1 - P$ confidence level: for example, the region above and to the right of the 0.1 contour is ruled out at the 90% confidence level

Table 5. Importance of the M Band Data

Star Name	Total simulated detections	2-band detections	L' -only detections	M -only detections
ϵ Eri	2850	46.98%	8.28%	44.74%
61 Cyg B	1610	52.73%	1.55%	45.71%
61 Cyg A	965	63.01%	22.80%	14.20%
ξ Boo B	157	61.15%	18.47%	20.38%
ξ Boo A	115	60.00%	18.26%	21.74%
GJ 702 A	9	22.22%	0.00%	77.78%

Note. — The usefulness of M band observations, based on our detailed Monte Carlo simulation. When M band observations were made of a given star, they did substantially increase the number of simulated planets detected around that star.

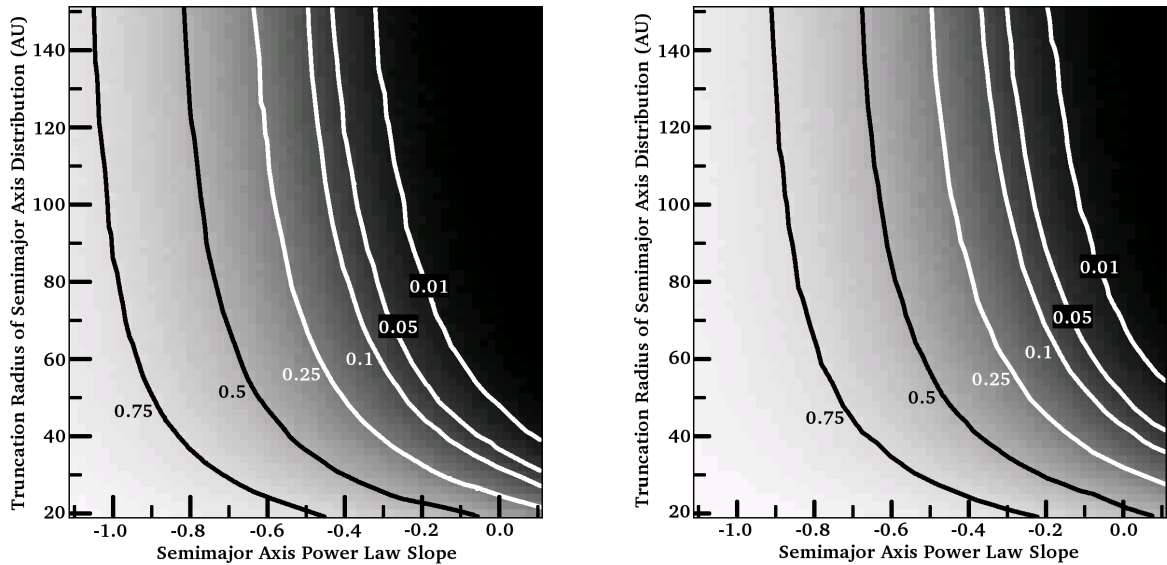


Fig. 2.— Probability of our survey detecting zero planets, as a function of the power law slope of the semimajor axis distribution β , where $\frac{dn}{da} \propto a^\beta$, and the outer truncation radius of the semimajor axis distribution. Here, the slope of the mass distribution α has been taken as -1.1 (left) and -1.51 (right), where $\frac{dn}{dM} \propto M^\alpha$. Since we found no planets, distributions that lead to a probability P of finding no planets are ruled out at the $1 - P$ confidence level: for example, the regions above and to the right of the 0.1 contours are ruled out at the 90% confidence level

10% turn up a null result, the probability is too high. It is adjusted in steps of ever-decreasing size until the correct value is reached.

Figure 3 shows the 90% confidence upper limit on $P(M, a)$ as a function of mass M and semimajor axis a . Each pixel represents thousands of realizations of our survey, with $P(M, a)$ finely adjusted to reach the correct value. Contours are overplotted showing where $P(M, a)$ is less than 8%, 10%, 25%, 50%, and 75%, with 90% confidence. Note that $P(M, a)$, the value constrained by our simulations, is a probability rather than a fixed fraction. The probability is the more scientifically interesting number, but is harder to constrain. For example, if 3.7% is the fraction of *the actual stars in our sample* that have planets with easy-to-detect properties, there are 2 such planets represented in our survey. However, if the *probability* of a star *like those in our sample* having such a planet is 3.7%, there is still a nonzero likelihood (13% chance) that *no star in our sample* actually has such a planet.

The results presented in Figure 3 can be interpreted as model-independent constraints on planet populations. For example, with 90% confidence we find that less than 50% of stars with properties like those in our survey have a 5 M_{Jup} or more massive planet in an orbit with a semimajor axis between 30 and 94 AU. Less than 25% of stars like those in our survey have a 7 M_{Jup} or more massive planet between 25 and 100 AU, less than 15% have a 10 M_{Jup} or more massive planet between 22 and 100 AU, and less than 12% have a 15 M_{Jup} or more massive planet/brown dwarf between 15 and 100 AU. These constraints hold independently of how planets are distributed in terms of their masses and semimajor axes.

HR 8799 appears to have a remarkable system of three massive planets, seen at projected distances of 24, 38, and 68 AU, with masses of roughly 10, 10, and 7 M_{Jup} , respectively (Marois et al. 2008). Using a Monte Carlo simulation like those used to create Figure 3, we find with 90% confidence that less than 8.1% of stars like those in our survey have a clone of the HR 8799 planetary system. For purposes of this simulation we adopted the masses above, and set the planets' orbital radii equal to their projected separations. Our 8.1% limit represents a step toward determining whether systems of massive planets in wide orbits are more common around more massive stars such as HR 8799 than FGK stars such as those we have surveyed.

3.6. Our Survey in the Big Picture

The surveys of Kasper et al. (2007) and Biller et al. (2007), have set constraints on the distributions of extrasolar planets similar to those we present herein, while the work of Nielsen et al. (2008) and especially Lafrenière et al. (2007) has set stronger constraints. The main importance of our work is that we targeted a different set of stars, at different wavelengths, and confirmed the conclusions of the other surveys.

Theoretical spectra of self-luminous extrasolar planets are very poorly constrained observationally. The recent detections of possible planets around HR 8799 (Marois et al. 2008), Fomalhaut

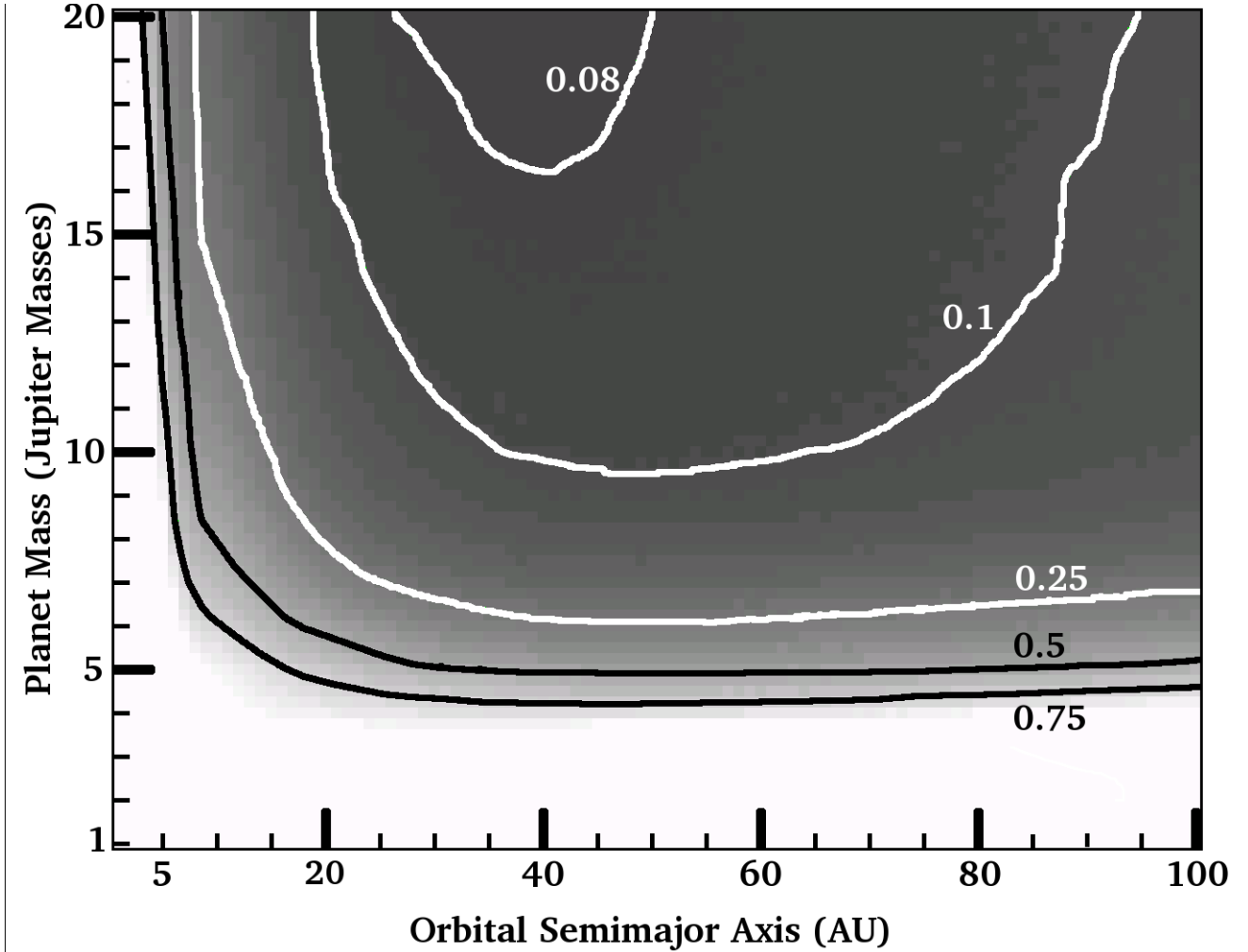


Fig. 3.— 90% confidence level upper limits on the probability $P(M, a)$ that a star like those in our survey will have a planet of mass M and semimajor axis a . This plot shows, for example, that our survey constrains the abundance of $10 M_{Jup}$ or more massive planets with an orbital semimajor axes between 22 and 100 AU to be less than 15% around sun-like stars. The abundance of $5 M_{Jup}$ or more massive planets between 25 and 94 AU is constrained to be less than 50%. The latter range does not extend all the way to 100 AU because our sensitivity to planets in very distant orbits decreases somewhat due to the possibility of their lying beyond our field of view.

(Kalas et al. 2008), and β Pic (Lagrange et al. 2009) are either single-band (β Pic) or only beginning to be evaluated at multiple wavelengths (HR 8799, Fomalhaut). The candidate planets orbiting HR 8799 and β Pic are hotter than we would expect to find orbiting middle-aged stars such as those in our survey, while HST photometry of Fomalhaut b suggests much of its brightness is starlight reflected from a circumplanetary dust disk. Our survey, and other exoplanet surveys, must therefore be interpreted using models of planetary spectra that are not yet well-tested against observations.

Such models predict brightnesses in the H band, and particularly in narrow spectral windows within the H band, that are enormously in excess of black body fluxes. The constraints set by the surveys of Masciadri et al. (2005); Biller et al. (2007); Nielsen et al. (2008); and Lafrenière et al. (2007) depend on the accuracy of these predictions of remarkable brightness in the H band. The L' and M bands that we have used are nearer the blackbody peaks of low-temperature self-luminous planets, and might be expected to be more reliable.

However, Leggett et al. (2007) and Reid & Cruz (2002) suggest that the M band brightness at least of hotter extrasolar planets will be less than predicted by Burrows et al. (2003) due to above-equilibrium concentrations of CO from convective mixing. Hubeny & Burrows (2007) present new models indicating the effect diminishes for cooler planets, but it would still have some effect on our M band sensitivity. It might actually enhance the L' brightness through line-blanketing. Theoretical spectra such as those of Burrows et al. (2003) may or may not be more reliable in the L' and M bands than at shorter wavelengths. However, so long as the models remain poorly constrained by observations at every wavelength, conclusions based on observations at multiple wavelengths will be more secure. Our survey, with that of Kasper et al. (2007), has diversified planet imaging surveys across a broader range of wavelengths.

In another sense our survey differs even from that of Kasper et al. (2007): we have investigated older stars. This is significant because planetary systems up to ages of several hundred Myr may still be undergoing substantial dynamical evolution due to planet-planet interactions (Juric & Tremaine 2007; Gomes et al. 2005). Our survey did not necessarily probe the same planet population as, for example, those of Masciadri et al. (2005) and Kasper et al. (2007). Finally, theoretical models of older planets are likely more reliable than for younger ones, as these planets are further from their unknown starting conditions and moving toward a well-understood, stable configuration such as Jupiter’s. It has been suggested by Marley et al. (2007), in fact, that theoretical planet models such as those of Burrows et al. (2003) and Baraffe et al. (2003) may overpredict the brightness of young (< 100 Myr) planets by orders of magnitude, while for older planets the models are more accurate.

We have focused on nearby, mature star systems, and have conservatively handled the ages of stars. This makes our survey uniquely able to confirm that the rarity of giant planets at large separations around solar-type stars, first noticed in surveys strongly weighted toward young stars, persists at older system ages. It is not an artifact of model inaccuracy at young ages due to unknown

initial conditions.

4. The Future of the L' and M Bands

In the L' and M bands, the sky brightness is much worse than at shorter wavelengths (e.g., the H band regime used by Biller et al. (2007) and Lafrenière et al. (2007)), but predicted planet/star flux ratios are better. Thus it makes sense to use these bands on bright stars, where the planet/star flux ratio is a more limiting factor than the sky brightness. In Heinze et al. (2008), we have shown that M band observations tend to do better than those at shorter wavelengths at small separations from bright stars.

The L' and M bands are also most sensitive relative to shorter wavelengths for detecting the lowest temperature planets, as these have the reddest $H - L'$ and $H - M$ colors. Such very low temperature planets can only be detected around the nearest stars, so it is for very nearby stars that L' and M band observations make the most sense. According to the Burrows et al. (2003) models, the most sensitive H -regime observations made to date (those of Lafrenière et al. (2007)) would have set better mass limits than our observations around all of our survey targets except the very nearest objects, such as ϵ Eri and 61 Cyg. At present, the H -regime delivers far the best planet detection prospects for most stars.

However, as detector technology improves, larger telescopes are built, and longer planet detection exposures are attempted, the sensitivity at all wavelengths will increase. This means that low-temperature planets, with their red IR colors, will be detectable at large distances, and the utility of the L' and especially the M bands will increase. In Figure 4 we show the minimum detectable planet mass for hypothetical stars at 5 and 10 pc distance as a function of the increase over current sensitivity in the H , L' , and M bands. We have taken current sensitivity to be $H = 23.0$ (i.e., Lafrenière et al. (2007)), $L' = 16.5$, and $M = 13.5$ (i.e., the present work, scaled to an 8m telescope such as Lafrenière et al. (2007) used). These are background limits, not applicable close to bright stars. Based on Heinze et al. (2008), we believe the L' and M bands will do even better relative to H closer to the star where observations are no longer background limited. We have deliberately chosen the characteristics of the hypothetical stars in Figure 4 to be less good than the best available planet search candidates, so that in each case a number of stars closer and younger than the example actually exist.

Figure 4 illustrates two very important points. First, with a relatively minor increase of 1-1.5 mag in sensitivity, the M band will be sensitive to considerably lower-mass planets around stars within 5 pc than can be detected with H band observations, even if the H band sensitivity increases the same amount. Second, the advantage of the M band decreases with increasing distance, but as larger telescopes and longer exposures increase sensitivities to 2.5 mag above present levels, the M band will be superior to H out to 10 pc. In fact, with an increase of 3 mag, M band will surpass H out to 25 pc. All this applies to background-limited observations. Close to bright stars, the

relative utility of the M band should be even higher. Figure 4 also suggests that the M band is considerably more promising than L' . Note that the predicted suppression of flux in the M band due to elevated levels of CO (Leggett et al. 2007; Reid & Cruz 2002) will not apply to planets at the low temperatures relevant for Figure 4. Though at present they are surpassed in sensitivity by H -regime observations for all but the nearest stars, the L' and especially the M bands hold considerable promise for the future.

5. Conclusion

We have surveyed unusually nearby, mature star systems for extrasolar planets in the L' and M bands using the Clio camera with the MMT AO system. By extensive use of blind sensitivity tests involving fake planets inserted into our raw data (reported in detail in our concurrently published Observations paper), we established a definitive significance vs. completeness relation for planets in our data, which we then used in Monte Carlo simulations to constrain planet distributions.

We set interesting limits on the masses of planets and brown dwarfs in the star systems we surveyed, but we did not detect any planets. Based on this null result, we place constraints on the power laws that may describe the distribution of extrasolar planets in mass and semimajor axis. We also place constraints on planet abundances independent of the distributions. If the distribution of planets is a power law with $dN \propto M^\alpha a^\beta dM da$, normalized to be consistent with radial velocity statistics, we rule out $\alpha = -1.1$ and $\beta = -0.46$, truncated at 110 AU, at the 90% confidence level. With the same confidence level we find that if $\alpha = -1.31$ and $\beta = 0.0$, the semimajor axis distribution must truncate at 38 AU or less. Independent of distribution models, with 90% confidence no more than 50% of sun-like stars such as those in our survey have a $5 M_{Jup}$ or more massive planet orbiting between 30 and 94 AU, no more than 15% have a $10 M_{Jup}$ planet orbiting between 22 and 100 AU, and no more than 25% have a $20 M_{Jup}$ object orbiting between 8 and 100 AU.

Our constraints on planet abundances are similar to those placed by Kasper et al. (2007) and Biller et al. (2007), but less tight than those of Nielsen et al. (2008) and especially Lafrenière et al. (2007). However, we have surveyed a more nearby, older set of stars than any previous survey, and have therefore placed constraints on a more mature population of planets. Also, we have confirmed that a paucity of giant planets at large separations from sun-like stars is robustly observed at a wide range of wavelengths.

The best current H regime observations, those of Lafrenière et al. (2007), would attain sensitivity to lower mass planets than did our L' and M band observations for all of our survey targets except those lying within 4 pc of the Sun. However, as larger telescopes are built and longer exposures are attempted, the sensitivity of M band observations may be expected to increase at least as fast as that of H band observations (in part because M band detectors are currently a less mature technology). A modest increase from current sensitivity levels, even if paralleled by

an equal increase in H band sensitivity, would render the M band the wavelength of choice for extrasolar planet searches around a large number of nearby stars.

6. Acknowledgements

This research has made use of the SIMBAD online database, operated at CDS, Strasbourg, France, and the VizieR online database (see Ochsenbein et al (2000)).

We have also made extensive use of information and code from Press et al. (1992).

We have used digitized images from the Palomar Sky Survey (available from http://stdatu.stsci.edu/cgi-bin/dss_form), which were produced at the Space Telescope Science Institute under U.S. Government grant NAG W-2166. The images of these surveys are based on photographic data obtained using the Oschin Schmidt Telescope on Palomar Mountain and the UK Schmidt Telescope.

Facilities: MMT, 61" Kuiper

REFERENCES

- Barrado y Navascués, D. 1998, *A&A*, 339, 831
- Baraffe, I., Chabrier, G., Barman, T. S., Allard, F., & Hauschildt, P. H. 2003, *A&A*, 402, 701
- Baraffe, I., Chabrier, G., Allard, F., Hauschildt, P. H. 1998, *A&A*, 337, 403
- Biller, B. A., Close, L. M., Masciadri, E., Nielsen, E., Lenzen, R., Brandner, W., McCarthy, D., Hartung, M., Kellner, S., Mamajek, E., Henning, T., Miller, D., Kenworthy, M., & Kulesa, C. 2007, *ApJS*, 173, 143
- Bouchy, F., Mayor, M., Lovis, C., Udry, S., Benz, W., Bertaux, J.-L., Delfosse, X., Mordasini, C., Pepe, F., Queloz, D., & Segransan, D. 2009, *A&A*, 496, 527
- Bryden, G., Beichman, C. A., Trilling, D. E., Rieke, G. H., Holmes, E. K., Lawler, S. M., Stapelfeldt, K. R., Werner, M. W., Gautier, T. N., Blaylock, M., Gordon, K. D., Stansberry, J. A., & Su, K. Y. L. 2006, *ApJ*, 636, 1098
- Burrows, A., Sudarsky, D., & Lunine, J. I. 2003, *ApJ*, 596, 578
- Butler, R. P., Wright, J. T., Marcy, G. W., Fischer, D. A., Vogt, S. S., Tinney, C. G., Jones, H. R. A., Carter, B. D., Johnson, J. A., McCarthy, C., & Penny, A. J. 2006, *ApJ*, 646, 505.
- Cohen, M., Walker, R. G., Michael, J. B., & Deacon, J. R. 1992, *AJ*, 104, 1650
- Cox, A. N. 2000, *Allen's Astrophysical Quantities* (Fourth Edition; New York, NY: Springer-Verlag New York, Inc.)

- Cumming, A., Butler, R. P., Marcy, G. W., Vogt, S. S., Wright, J. T., & Fischer, D. A. 2008, *PASP*, 120, 531.
- Cutri, R., Skrutskie, M., van Dyk, S., Beichman, C., Carpenter, J., Chester, T., Cambresy, L., Evans, T., Fowler, J., Gizis, J., Howard, E., Huchra, J., Jarett, T., Kopan, E., Kirkpatrick, J., Light, R., Marsh, K., McCallon, H., Schneider, S., Stiening, R., Sykes, M., Weinberg, M., Wheaton, W., Wheelock, S., & Zacarias, N. 2003, 2MASS All Sky Catlog of point sources (The IRSA 2MASS All-Sky Point Source Catalog, NASA/IPAC Infrared Science Archive. <http://irsa.ipac.caltech.edu/applications/Gator/>)
- Favata, F., Micela, G., Sciortino, S., & D’Antona, F. 1998, *A&A*, 335, 218
- Fischer, D. 1998, PhD Thesis entitled **Lithium Abundances in Field K Dwarfs**, University of California Santa Cruz
- Fischer, D. A. & Valenti, J. 2005, *ApJ*, 622, 1102
- Freed, M., Hinz, P., Meyer, M., Milton, N., & Lloyd-Hart, M. 2004, *Proc. SPIE*, 5492, 1561
- Gomes, R., Levison, H., Tsiganis, K., & Morbidelli, A. 2005 *Nature*, 435, 466
- Heinze, A. N., Hinz, P. M., Kenworthy, M., Miller, D., & Sivanandam, S. 2008, *ApJ*, 688, 583
- Hinz, P., Heinze, A., Sivanandam, S., Miller, D., Kenworthy, M., Brusa, G., Freed, M., & Angel, J. 2006, *ApJ*, 653, 1486.
- Hubeny, I. & Burrows, A. 2007, *ApJ*, 668,1248
- Hünsch, M., Schmitt, J., Sterzik, M. & Voges, W. 1998, *Astron. Astrophys. Suppl. Ser.* 135, 319
- Juric, M. & Tremaine, S. 2007, *ArXiv e-prints*, astro-ph/0703.0160
- Kalas, P., Graham, J., Chiang, E., Fitzgerald, M., Clampin, M., Kite, E., Stapelfeldt, K. Marois, C., & Krist, J. 2008, *Science*, 322, 1345
- Karatas, Y., Bilir, S., & Schuster, W. 2005, *MNRAS*, 360, 1345
- Kasper, M., Apai, D. Janson, M. & Brandner, W. 2007, *A&A*, 472, 321
- Kenworthy, M., Codona, J., Johanan, L., Hinz, P., Angel, J., Heinze, A., & Sivanandam, S. 2007, *ApJ*, 660, 762
- King, J., Villarreal, A., Soderblom, D., Gulliver, A., & Adelman, S. 2003, *ApJ*, 125,1980
- Lafrenière, D., Doyon, R., Marois, C., Nadeau, D., Oppenheimer, B., Roche, P., Rigaut, F., Graham, J., Jayawardhana, R., Johnstone, D., Kalas, P., Macintosh, B., & Racine, R. 2007, *ApJ*, 670, 1367

- Lagrange, A.-M., Gratadour, D., Chauvin, G., Fusco, T., Ehrenreich, D., Mouillet, D., Rossuet, G., Rouan, D., Allard, F., Gendron, È., Charton, J., Mugnier, L., Rabou, P., Montri, J., & Lacombe, F. 2009, *A&A*, 493, 21
- Leggett, S., Saumon, D., Marley, M., Geballe, T., Golimowski, D., Stephens, D., & Fan, X. 2007, *ApJ*, 655, 1079
- López-Santiago, J., Montes, D., Crespo-Chac/’on, I., & Fernández-Figueroa, M. J. 2006, *ApJ*, 643, 1160
- Lowrance, P., Becklin, E., Schneider, G., Kirkpatrick, J., Weinberger, A., Zuckerman, B., Dumas, C., Beuzit, J., Plait, P., Malumuth, E., Heap, S., Terrile, R., & Hines, D. 2005, *AJ*, 130, 1845
- Marley, M. S., Fortney, J. J., Hubickyj, O., Bodenheimer, P., & Lissauer, J. J. 2007, *ApJ*, 655, 541
- Marois, C., Lafrenière, D., Doyon, R., Macintosh, B., & Nadeau, D. 2006, *ApJ*, 641, 556
- Marois, C., Macintosh, B., Barman, T., Zuckerman, B., Song, I., Patience, J., Lafrenière, D., & Doyon, R. 2008, *Science*, 322, 1348
- Masciadri, E.; Mundt, R.; Henning, Th.; Alvarez, C.; & Barrado y Navascués, D 2005, *ApJ*, 625, 1004
- Montes, D., López-Santiago, J., Fernández-Figueroa, M., & Gálvez, M. 2001, *A&A*, 379, 976
- Mugrauer, M., Neuhaeuser, R., Guenther, E. W., Hatzes, A. P., Huelamo, N., Fernandez, M., Ammler, M., Retzlaff, J., Koenig, B., Charbonneau, D. Jayawardhana, R., & Brandner, W. 2004, *A&A*, 417, 1031
- Nielsen, E. L., Close, L. M., Biller, B. A., Masciadri, E., & Lenzen, R. 2008, *ApJ*, 674, 466
- Ochsenbein, F., Bauer, P. & Marcout, J. 2000, *ApJS*, 143, 230
- Potter, D., Cushing, M., & Neuhauser, R. 2003, *csss*, 12, 689
- Perryman, M., Lindegren, L., Kovalevsky, J., Hog, E., Bastian, U., Bernacca, P., Creze, M., Donati, F., Grenon, M., Grewing, M., Van Leeuwen, F., Van Der Marel, H., Mignard, F., Murray, C., Le Poole, R., Schrijver, H., Turon, C., Arenou, F., Froeschle, M., & Peterson, C. 1997, *A&A*, 323, L49
- Press, W. H., Teukolsky, S.A., Vetterling, W. T., & Flannery, B. P. 1992, *Numerical Recipes in C* (Second Edition; New York, NY: Cambridge University Press)
- Reid, I. & Cruz, K. 2002, *AJ*, 123, 466
- Sivanandam, S., Hinz, P., Heinze, A., & Freed, M. 2006, *Proc. SPIE*, 6269, 27

- Song, I., Zuckerman, B., & Bessell, M. 2003, *ApJ*, 599, 342
- van Dokkum, P. G. 2001, *PASP*, 113, 1420
- Wichmann, R., Schmitt, J., & Hubrig, S. 2003, *A&A*, 399, 983
- Wichmann, R. & Schmitt, J. 2003, *MNRAS*, 342, 1021
- Zuckerman, B., Song, I., Bessell, M., & Webb, R. 2001, *ApJ*, 562, L87

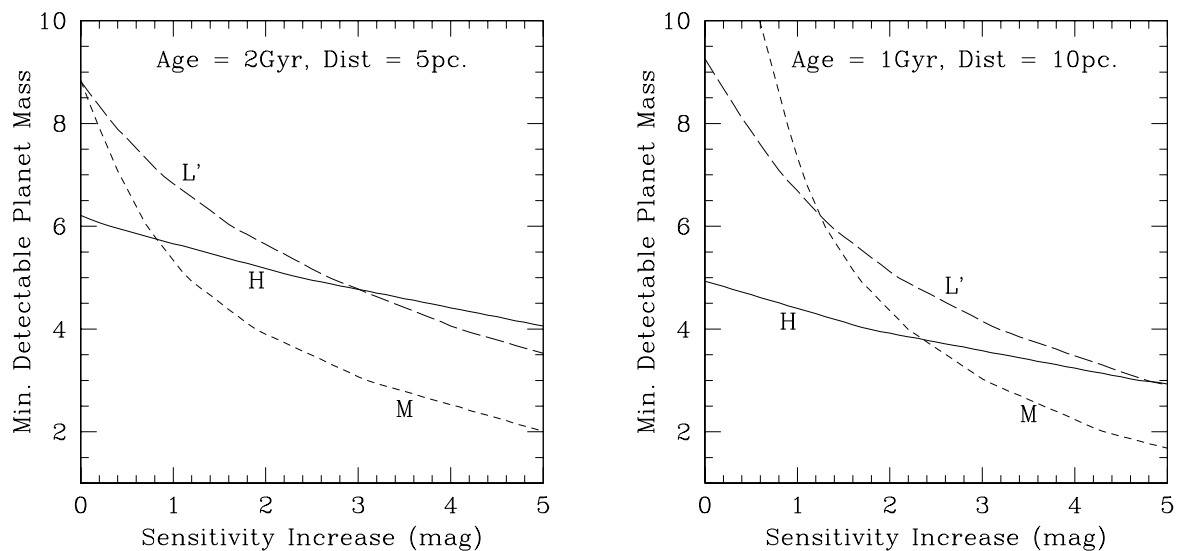


Fig. 4.— Minimum detectable planet mass in units of M_{Jup} for stars at 5pc (left) and 10pc (right), in the H , L' , and M bands, as a function of increase over current sensitivity. We have taken current sensitivities to be $H = 23.0$, $L' = 16.5$, and $M = 13.5$. Modest increases over current sensitivities will render the M band very promising relative to shorter wavelengths, especially for nearby stars.